Journal of Marine Research, 53, 1059–1080, 1995

An estimate of the climatological mean circulation in the western North Atlantic

by Wei Wang[1,2] and M. Susan Lozier[1]

ABSTRACT

In order to produce a long-term mean circulation pattern for the western North Atlantic, geostrophic velocities have been calculated using a recently-assembled hydrographic database comprised of NODC station data from 1904–1990. The property fields generated from this database are smoothed on isopycnal surfaces and have a nominal resolution of one degree for the spatial domain of this study (34–42N, 48–66W). To reference the geostrophic velocities, SOFAR float data over the period 1972–1990 are used. The flow fields from this calculation are compared to fields produced using an assumed level of no motion. The calculations employing float data yield a flow field with two strong northern cyclonic gyres separated at ~56W, the approximate location of the New England Seamounts. The southern anticyclonic recirculation gyre is larger and weaker with two weak cells embedded within it. Significant downstream changes in transport result from the presence of the recirculations, particularly the northern gyres.

1. Introduction

Despite the relatively dense sampling of the North Atlantic, the long-term mean circulation of the basin is poorly understood in some regions. This is particularly true for the recirculations associated with the Gulf Stream in the western portion of the basin. An understanding of the structure, extent and strength of these recirculations is crucial to efforts that are aimed at partitioning the Gulf Stream transport into that driven by thermohaline, wind and inertial processes. After several decades of observations, there is a general consensus that the eastward-flowing Gulf Stream is flanked both to the north and south by significant recirculations. However, the number of recirculating gyres and the spatial extent of these gyres remains an open question. A recent scheme by Hogg (1992), based on a compilation of transport measurements, proposes a single gyre structure for each of the northern and southern domains. The southern gyre, reminiscent of that proposed by Worthington (1976), extends from near the bifurcation of the Gulf Stream, at the Tail of the Grand Banks, to Cape Hatteras. The proposed northern recirculation is more

1. Ocean Sciences Program, Duke University, Durham, North Carolina, 27708, U.S.A.
2. Present address: Lamont Doherty Earth Observatory, Columbia University, Palisades, New York, 10964, U.S.A.

confined, situated between the Tail of the Grand Banks and the New England Seamount Chain (NESC). In contrast to this scheme, Schmitz and McCartney (1993), from a synthesis of historical observations, propose a two-gyre structure for each of the northern and southern recirculations, with each set of gyres roughly divided by the NESC. For the northern case the western gyre is in agreement with the work of Csanady and Hamilton (1988), who propose a well-defined cyclonic gyre west of the NESC, in addition to the cyclonic gyre east of the seamounts described by Hogg (1992). Thus, circulation schemes based on observations are not consistent in their description of the western North Atlantic.

Inverse models of the North Atlantic, which have become increasingly sophisticated since Wunsch (1978) first applied inverse techniques to ocean hydrographic data, have combined dynamics with data to produce circulation patterns in this basin. Earlier efforts to establish the long-term mean circulation in this locale have been limited by the use of synoptic (rather than long-term mean) hydrographic data (Wunsch and Grant, 1982; Mercier, 1989). More recently, Martel and Wunsch (1993) have constrained the North Atlantic circulation with a hydrographic database compiled by Fukumori and Wunsch (1991), which spans the temporal domain 1981–1985, in their effort to produce a "blurred snapshot" of a synoptic Gulf Stream. Mercier *et al.* (1993) combine this dataset with the synoptic sections from both IGY and Gulf Stream '60 data in their inversion of the North Atlantic. Thus, they essentially use hydrographic data collected from two five-year periods to produce a mean flow field. Despite the relative abundance of hydrographic data during these time periods, substantial smoothing (on the order of 500 km) is still required to produce hydrographic properties for each grid element in these inverse models. Thus, the resolution of smaller scale features such as the Gulf Stream recirculations, becomes more difficult.

Recently a new climatological hydrographic database has been introduced for the North Atlantic (Lozier *et al.*, 1995). This database was compiled using historical station data from the National Oceanic Data Center and differs from the Levitus (1982) database in three important regards. First the database spans the temporal domain 1904–1990, thus including 60% more data than Levitus used in the North Atlantic. Secondly, the properties are averaged and smoothed on isopycnal surfaces rather than on surfaces of constant depth, as Levitus chose. As described by Lozier *et al.* (1994) this choice eliminates the introduction of sizable temperature and salinity anomalies into the database. The third and most important change, in regard to this work, is the order of magnitude increase in the resolution of the mean fields. Because of the increase in the amount of data, and because smoothing scales were set by local data density rather than selected uniformly for the global ocean, the resolution of this database is nominally 1 degree. This compares to smoothing scales on the order of 1000 km for the Levitus atlas. As detailed by Lozier *et al.* (1995), this new database

has revealed new features in the pressures, temperature and salinity fields, particularly on isopycnal surfaces in the intermediate and deep waters.

Because this database offers high resolution property fields on climatological time scales, it can potentially serve as the hydrographic database in sophisticated inverse models to establish a long-term mean (i.e. over several decades) of the North Atlantic. To get a preliminary look at what circulation features might be resolved with this database, we present the results in this paper of a simple geostrophic calculation using the hydrography in conjunction with SOFAR float data and, in another case, in conjunction with an assumed level of no motion. SOFAR float data, which were collected over a span of approximately 20 years, were chosen in order to use absolute velocities averaged over a length comparable to the hydrographic data. With the use of a database averaged over many decades there is the uncertainty as to what the "average circulation" represents. It certainly is *not* an average synoptic circulation pattern, particularly in areas of strong temporal variability, such as the Gulf Stream. Thus, the objective for establishing such a circulation lies primarily with placing a climatological Gulf Stream in a geographic context and in forming a basis from which variability can be judged. Finally, we note that this work is the first test of the new database in a dynamic calculation and is not intended to be definitive or comprehensive. In this paper we detail our efforts toward producing the average circulation pattern for the western North Atlantic. Data sources and methods are discussed in Sections 2 and 3, respectively. Results are discussed in Section 4, transport calculations are presented in Section 5, followed by a summary in Section 6.

2. Data

a. Hydrographic data. The mean hydrographic properties of the North Atlantic compiled by Lozier *et al.* (1995) were used for the geostrophic calculations in this work. These means were constructed from 87 years (1904–1990) of hydrographic station data archived at the National Oceanic Data Center (NODC). Figure 1 shows the distribution of the approximately 134,000 stations that comprise this database. For the purpose of this study, the mean pressure, temperature and salinity were computed on 25 isopycnal surfaces distributed between the sea surface and approximately 4500 m. The vertical resolution of these surfaces is approximately equivalent to the standard levels used by Levitus (1982). Briefly, hydrographic properties from station data were projected onto a chosen isopycnal surface and then spatially averaged and smoothed on that surface, with the scale set by the local data density. In the Gulf Stream region a nominal resolution of one-degree was achieved, which is approximately an order of magnitude smaller than the resolution of the Levitus (1982) atlas. Further details of the data processing can be found in Lozier *et al.* (1995).

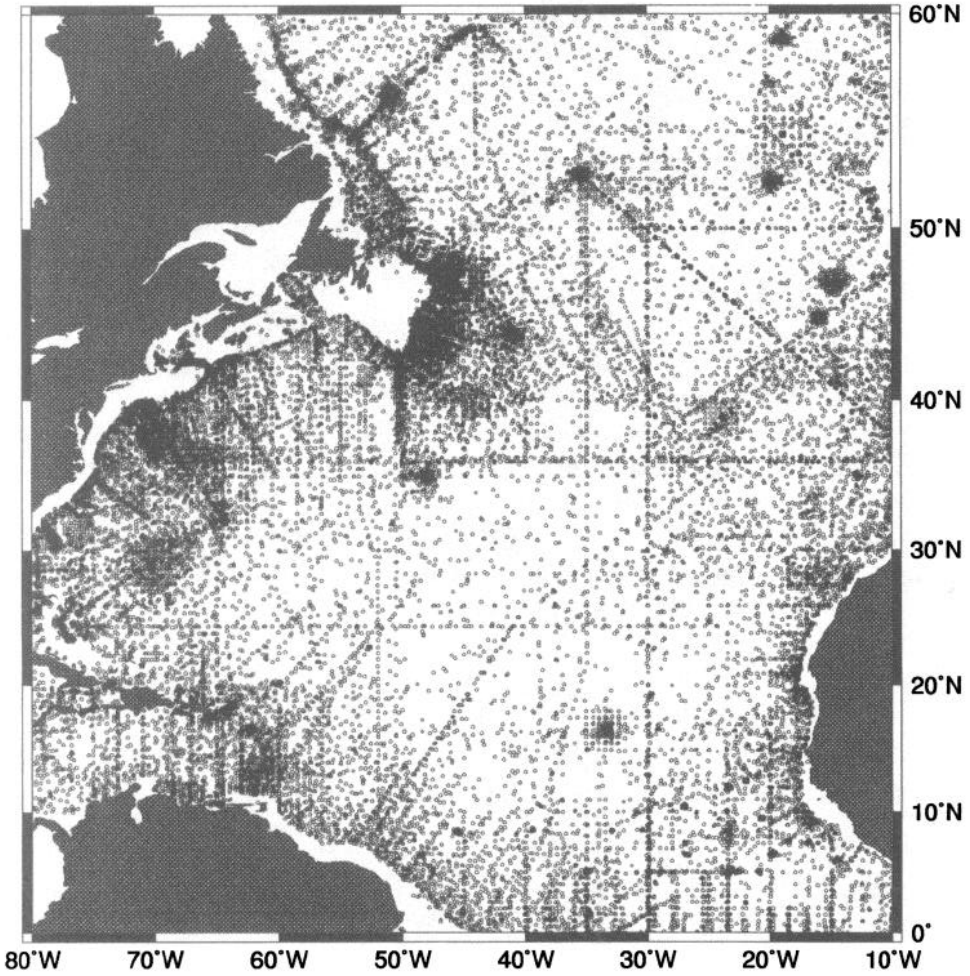

Figure 1. Hydrographic stations collected in the North Atlantic during 1904–1990 (from NODC archives), which are used to construct the mean property fields used in the geostrophic calculations.

b. Velocity data. From a collection of SOFAR floats that were released in the Gulf Stream region from 1972 to 1990, Owens (1991) constructed mean velocity fields in the western North Atlantic at depths of 700 m, 1500 m and 2000 m, the nominal depths of float release during this nineteen-year period. By treating the floats as roving current meters, equivalent Eulerian means were computed for the zonal and meridional velocities. Details of the calculations are given in Owens (1991). For our study the 1500 m floats were eliminated based on their limited spatial coverage. In order to be compatible with the isopycnal-averaged hydrographic data, it is desired to have the reference velocities also lie on an isopycnal. However, because no vertical

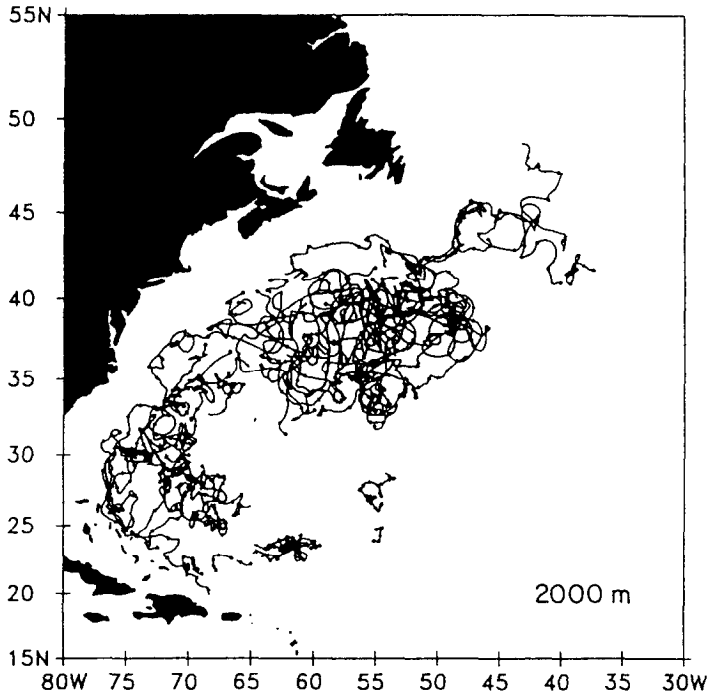

Figure 2. Trajectories of SOFAR floats at a nominal depth of 2000 m. (Fig. 4 from Owens, 1991).

shear information is available from the isobaric floats, the instantaneous float velocities could not be interpolated onto an isopycnal. Since the isopycnal slopes at 2000 m are quite small and (consequently) the velocity shear at that depth is quite weak, we make the assumption that the 2000 m float velocities lie approximately on the $\sigma_2 = 36.93$ surface, which has a nominal depth of 1990 m and a rise of 350 m over the Gulf Stream. A similar assumption for the 700 m floats would place the float velocities on the $\sigma_1 = 31.80$ surface, which has a mean depth of 694 m over our domain. However, the slope for this thermocline surface is considerably larger (31.80 has a rise of approximately 600 m over the Gulf Stream) than the isopycnal slope near 2000 m. Thus, mapping the 700 m floats onto the 31.80 isopycnal is not reasonable given the stronger vertical shear in the thermocline. For this reason we opted to use only the 2000 m floats (Figure 2, from Owens (1991)) to reference the geostrophic velocities.

Based on the spatial extent of the SOFAR floats at 2000 m we chose the domain bounded by 48–66W and 34–42N for our calculations (Fig. 3). Within this domain the hydrographic properties were computed from a total of 4312 hydrographic stations. Hydrographic data were available for each one degree grid element in our domain.

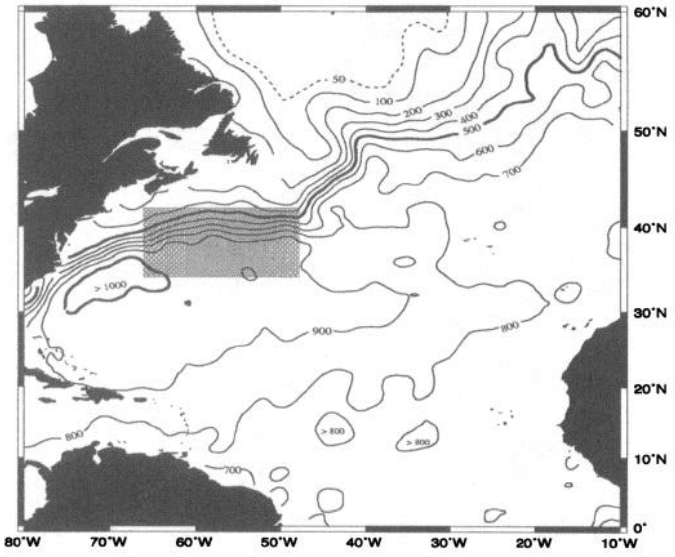

Figure 3. Calculation domain (shadowed box). Marked on the contours are depths (in decibars) of the isopycnal surface $\sigma_1 = 31.85$.

The few velocity blanks in our chosen domain were filled by a 5th-order polynomial interpolation of the surrounding float data.

3. Methods

A vertically-integrated version of the thermal wind equation, adapted for surfaces of constant potential density (Zhang and Hogg, 1992), is used for the calculations in this study:

$$\mathbf{k}xf(\mathbf{u} - \mathbf{u}_r) = -[\nabla_s(p'\delta - p'_r\delta_r) - \nabla_s \int_{pr}^{p} \delta dp] + [p'\nabla\delta - p'_r\nabla\delta_r], \qquad (1)$$

where $\mathbf{u} = (u, v)$ is the horizontal velocity vector, f is the Coriolis parameter, $\mathbf{k}$ is the unit vector normal to the isopycnal, δ is the specific volume anomaly and p' is the pressure anomaly on an isopycnal surface ($p' = p - \bar{p}$, were $\bar{p}$ is the mean pressure of the isopycnal surface). The subscripts r and s are used to denote the reference values and differentiation along an isopycnal surface, respectively. This differs from the traditional formulation of a Montgomery streamfunction in the use of the pressure anomaly, rather than the pressure, of a chosen isopycnal. This choice considerably reduces the magnitude of the last term on the right hand side of the equation, which is the error term when the streamfunction is defined on an isopycnal surface. We have adopted Zhang and Hogg's formulation (referred to as a pressure

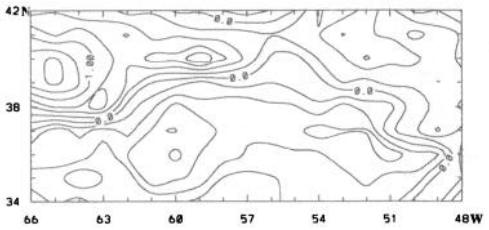

Figure 4. The streamfunction field calculated from the 2000 m float velocities. Contour interval is .25 $cm^2\ sec^{-2}$.

anomaly streamfunction) whereby:

$$\psi = p'\delta - \int^{p} \delta dp \qquad \text{and} \tag{2}$$

$$fu = -\partial\psi/\partial u \qquad \text{and} \qquad fv = \partial\psi/\partial x. \tag{3}$$

Since the Coriolis parameter varies by only 20% over our study domain, the pressure anomaly streamfunction behaves approximately as the usually-defined streamfunction, such that the velocity field can be inferred from its map. (Hereafter the pressure anomaly streamfunction will be referred to as *the* streamfunction.) With this definition Eq. (1) becomes:

$$\psi - \psi_r = \int_{p}^{pr} \delta dp + p'\delta - p_r'\delta_r. \tag{4}$$

Eq. (4) is used to calculate the streamfunction at each grid on all selected surfaces. Once a reference level is chosen, all terms on the right-hand side of Eq. (4) are obtained from the hydrographic data. As mentioned earlier, for the calculations involving the float data, a reference surface of $\sigma_2 = 36.93$ was chosen. For the level of no motion calculations, the $\sigma_4 = 45.90$ surface was chosen, which has a nominal depth of 4400 m. Although this surface rises $\sim$200 m across the Gulf Stream, we expect the absolute flow on this surface to be quite small relative to the thermocline flow. We are presenting this level of no motion case as a contrast to the calculation with the float data rather than as a realistic calculation. The specific volume anomaly in Eq. (4) is calculated from the mean hydrographic properties (P, T, and S) on the 25 isopycnal surfaces, and the integration in Eq. (4) is performed using those values. The last term on the right-hand side, $p_r'\delta_r$, is calculated at the chosen reference surface.

The unknown reference streamfunction, ψ_r, needed in Eq. (4), is calculated from the known float velocities using a discretization of Eq. (3). Centered differences on a one degree grid are used to represent the spatial derivatives of ψ. The known velocities are at the center of each grid, while the streamfunction variables are at the corners. For this even-determined system a simple inversion yields the *reference*

streamfunction field, shown in Figure 4. This field has been derived solely from the float velocities at 2000 m and is used in Eq. (4) to determine the absolute streamfunction at other levels. For the level of no motion computation, ψ_r was set equal to zero at all grids on the $\sigma_4 = 45.90$ surface.

The streamfunctions on selected isopycnals were calculated directly from Eq. (4) for each grid once ψ_r had been determined. The resultant streamfunctions on each surface were smoothed zonally with a three-point filter to reduce noise. Due to a concern of widening the Gulf Stream, no meridional smoothing was performed. Finally, geostrophic velocities were calculated from the smoothed streamfunction fields using Eq. (3).

4. Results

a. Geostrophic flow of the Gulf Stream and its recirculations. Results of the geostrophic calculation using the 2000 m float velocities and the isopycnal-averaged hydrographic data are shown on five representative isopycnal surfaces in Figure 5(a–e). From a comparison with Figure 4, it is evident how strongly the reference velocity influences the lower three surfaces. At these depths, where the vertical shear is weak, the reference velocity pattern and strength are projected almost entirely onto the deep surfaces. To separate the influence of the reference velocity field from the information contained in the hydrographic data we also present in this section the absolute streamfunction fields produced using a level of no motion. Again, this calculation assumes that ψ_r in Eq. (4) is equal to zero for all grids on the surface $\sigma_4 = 45.90$, which has a nominal depth of 4400 m. The streamfunction fields from this calculation are shown in Figure 5(f–j) for the surfaces corresponding to those in Figure 5(a–e).

For the calculation employing the float data, an eastward Gulf Stream is evident throughout the water column, with recirculation gyres flanking the stream to the north and south. Along the northern edge of the cyclonic recirculations a consistent westward flow exists throughout the deep ocean (Fig. 5d and e). This westward flow is particularly evident on the $\sigma_4 = 45.90$ and is interpreted as the Deep Western Boundary Current (DWBC). The southern recirculation is evident at all depths. In the upper ocean, this recirculation is broad and well-defined, but in the deep ocean, it consists of a number of weak localized gyres, such as the one near 61W. The resolution of these deep gyres is set by the density of the SOFAR float data, with the representativeness of this data discussed by Owens (1991). The northern recirculation is most evident on the surface $\sigma_1 = 31.80$ and those deeper. Two cyclonic systems, separated at 56W, comprise this recirculation. The western cyclone has a strong cell located west of 62W, and a weaker one centered at 59W. This western cyclonic system resembles the cyclonic slope gyre proposed by Csanady and Hamilton (1988) to exist solely in the upper waters of the slope area northeast of Cape Hatteras. Our calculation suggests that this western slope gyre is not surface-limited,

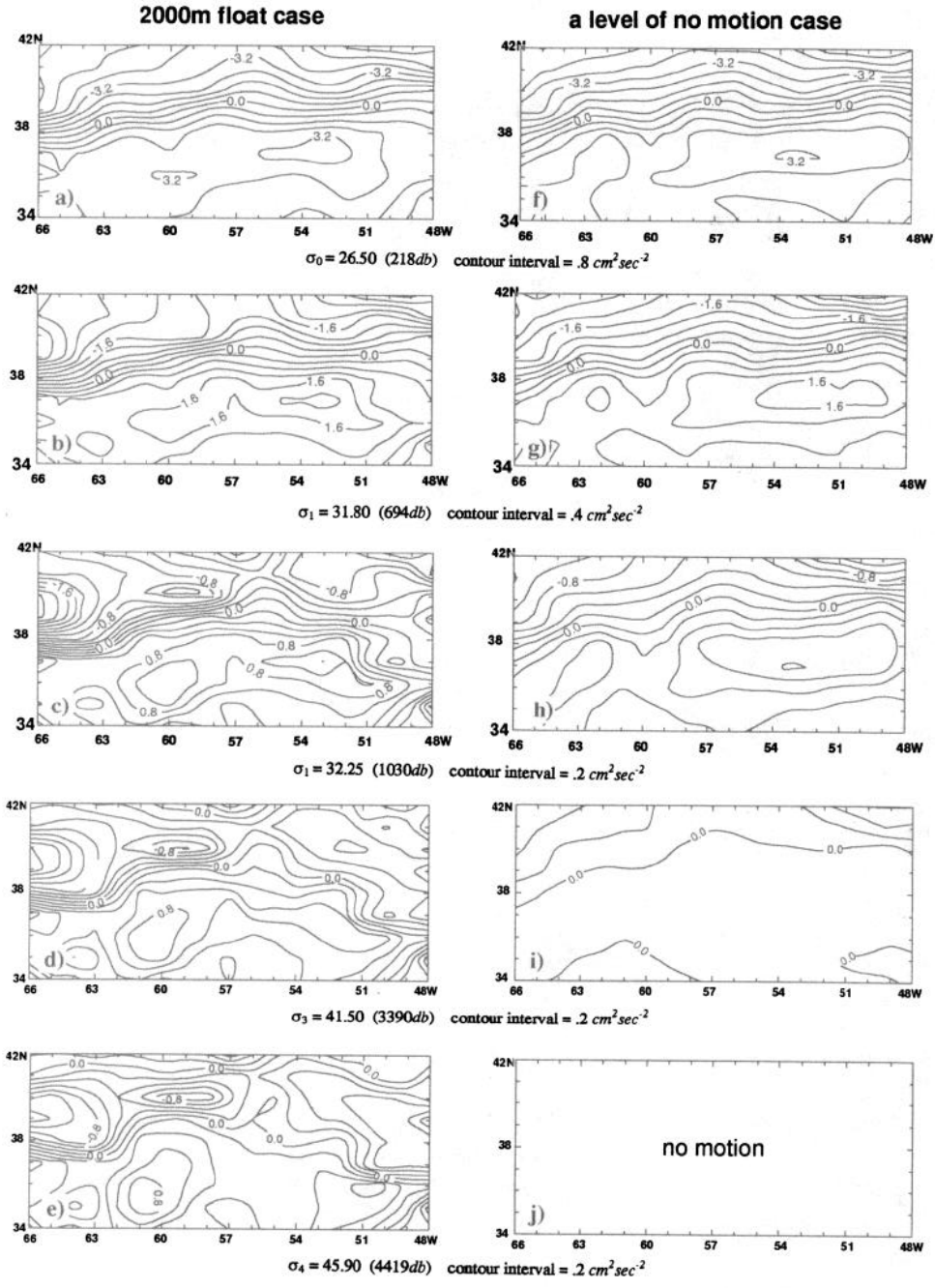

Figure 5. (a–e) Streamfunction fields from the calculation using isopycnal-averaged hydrographic fields and the reference velocities at 2000 m shown for representative surfaces, as marked. The numbers in parentheses represent the mean depth of the isopycnal and the subscript on the σ value is used to denote the reference pressure (in thousand of decibars). (f–j) Same as for (a–e) except that a level of no motion at $\sigma_4 = 45.90$ was used.

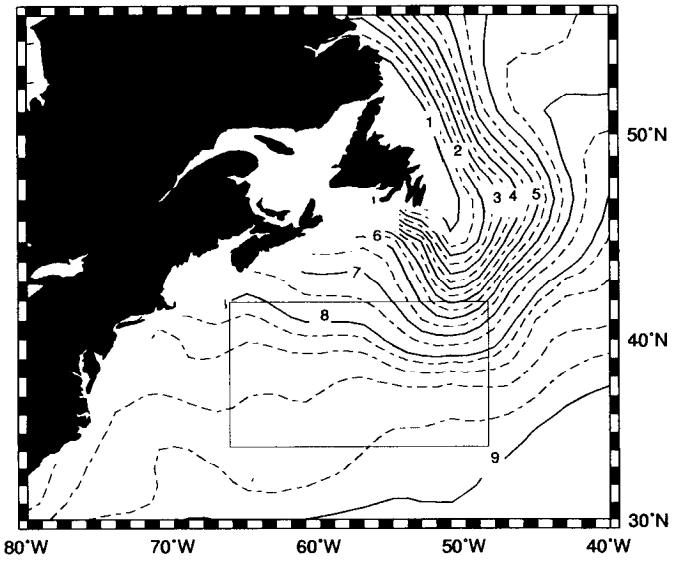

Figure 6. Potential temperature (°C) on the σ_1 = 31.80 surface from the Lozier *et al.* (1995) database. The box shows the domain used for the calculation of the geostrophic velocities.

but instead has a strong deep expression, which is clearly imposed by the reference velocity. The eastern cyclonic gyre seen north of the Stream resembles the cyclonic gyre in Hogg's (1992) western North Atlantic circulation model, which is believed to be associated with intrusions of the Labrador Current coming from the north. A map of potential temperature on the σ_1 = 31.80 surface (Fig. 6) shows that the waters in the eastern portion of our domain are considerably cooler than the waters to the west for the region north of the Gulf Stream. These cool waters, which are also high in oxygen and low in salinity (Lozier *et al.*, 1995), are apparently part of the Mixed Waters (Worthington, 1976) that are carried by the Labrador Current at this depth. In contrast, the warmer, saltier and lower oxygen waters (Lozier *et al.*, 1995) that occupy the western cyclonic gyre are seen to stem from the Gulf Stream system. Thus, from the temperature map it is concluded that the two northern cyclones contain different watermasses on the 31.80 surface. This watermass contrast is also seen on other thermocline surfaces, whereas below the thermocline ($\sim$1500 m) watermass differences between these two gyres cannot be made (Lozier *et al.*, 1995).

Removing the float velocities from the calculation creates large (and predictable) changes in the calculated flow fields, as seen in Figure 5(f–j). With an assumed level of no motion for the deepest surface the deep ocean is now left with only the weak hydrographic shear to define a baroclinic velocity, as seen on the σ_3 = 41.50 surface (Fig. 5i). The upper surface (σ_0 = 26.50, Fig. 5f) does not differ dramatically in either strength or pattern. The same is true of the next surface shown (σ_1 = 31.80, Fig. 5g), except the divergence to the north and convergence to the south near 57N are much

more pronounced than in Figure 5b. For the $\sigma_2 = 32.25$ surface (Fig. 5h), the effects of the reference velocity clearly dominate. The scale of the flow structure is much smaller with the float data included and the velocities are larger. However, it is important to note that without any float information included there is still a signature of a northward divergence from the Stream near 58N and a southward convergence into the Stream near 55W, thus creating a relative minimum in Stream width near ~56–57W.

To further examine these calculated flow fields, four meridional sections across the selected domain are displayed in Figures 7 and 8, for the velocities using the float data and those using a level of no motion, respectively. For completeness, velocities have been linearly extrapolated to the sea surface and to 4500 m using values from the two shallowest and deepest isopycnals, respectively. As expected the strongest differences in these fields are in the deep ocean. The relatively stronger shear in the thermocline waters dominates the imposed barotropic velocities in both cases to produce similar profiles in the upper 1000 m. However, the imposition of zero flow at depth essentially erases motion below the thermocline whereas the use of float data introduces some rich structure. In Figure 7, the core of the Gulf Stream is concentrated in the upper 1000 m, where the high velocity core is characterized by the familiar offshore tilting of its axis in all sections except for the one at 60.5W. This upper core of the Gulf Stream in these sections is seen to migrate to the north in the downstream direction, representing the northeast orientation of the mean Gulf Stream path. This climatological Gulf Stream spans a width of approximately 4 to 5 degrees of latitude, compared to an instantaneous width of approximately 1 to 1.5 degrees of latitude. Such smearing is mainly attributed to the temporal meandering of the Gulf Stream envelope, which has been estimated to be on the order of 500 km (Fuglister, 1963; Auer; 1987 and Cornillon, 1986). The Gulf Stream decelerates as it flows eastward with an attendant decrease in vertical shear, especially from the 60.5W to the 55.5W section. However, the shear at 50.5W is stronger than that at 55.5W, which is attributed to the local recirculation structure. A significant eastward flow extends to the deep ocean (down to 4500 m) in the western portion of our domain, namely in the 65.5W and 60.5W sections. In these two sections the deep Gulf Stream is situated beneath the surface Gulf Stream and has a robust flow as large as ~12 cm/sec. This deep expression weakens considerably by 55.5W, which is the approximate longitude of the split between the two northern recirculation gyres. As evident in Figure 4 the Gulf Stream deep flow is much weaker at this longitude due to the strong divergence to the north of some Gulf Stream waters.

A curious and strong bottom-intensified, eastward flow (as high as 10 cm/sec) appears in the 50.5W section. This flow results from the float velocities and can be seen in plan view in Figure 4. From the streamfunction map it appears that the deep Gulf Stream turns southeastward at approximately 54-53W and then (near 51W) continues eastward along the latitude 36.5N. The starting point of this concentrated

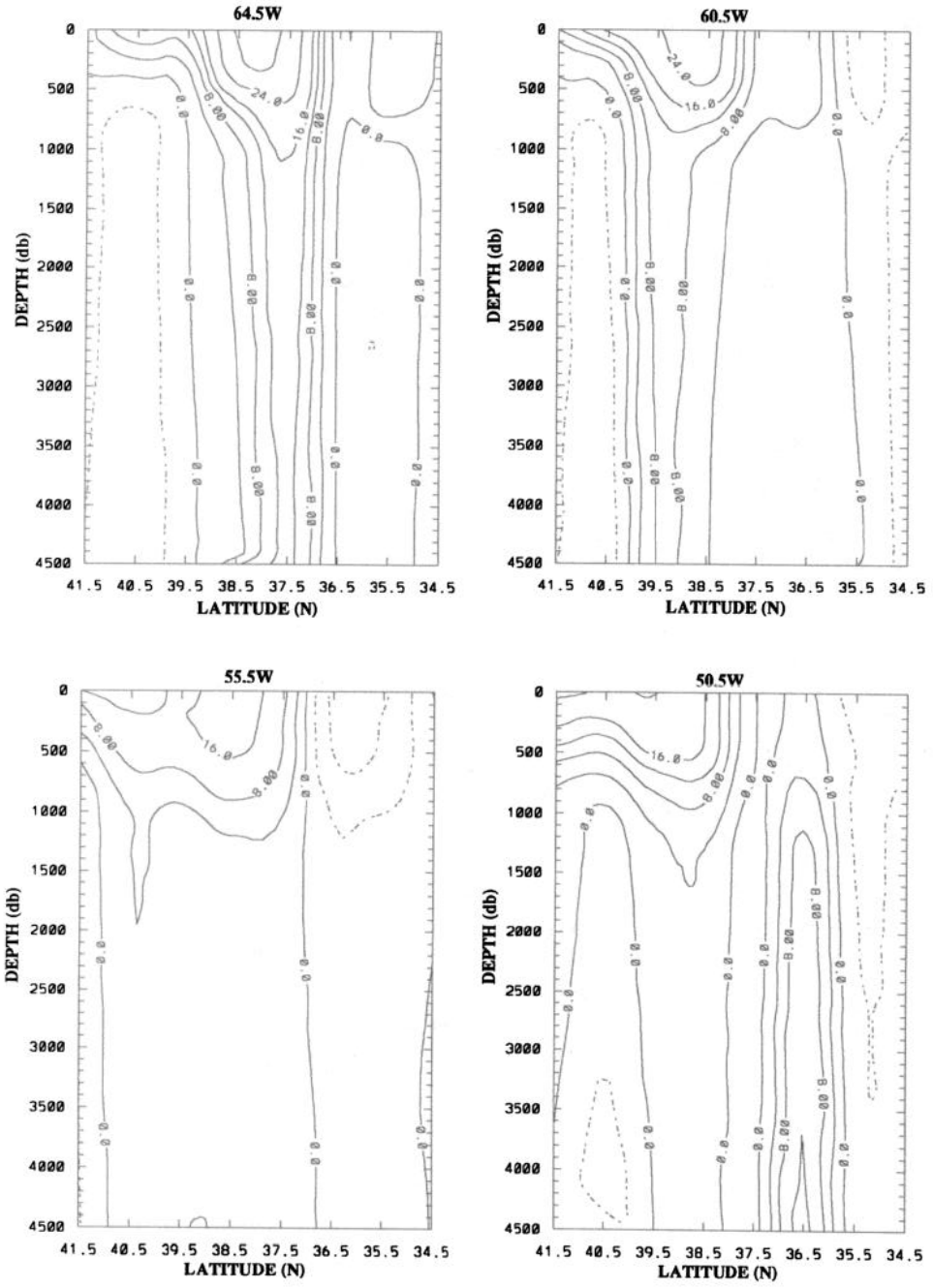

Figure 7. Meridional sections of zonal velocities from the calculation using isopycnal-averaged hydrographic fields and the reference velocities at 2000 m. Positive values are eastward velocities with a contour interval of 4 cm sec^{-1}.

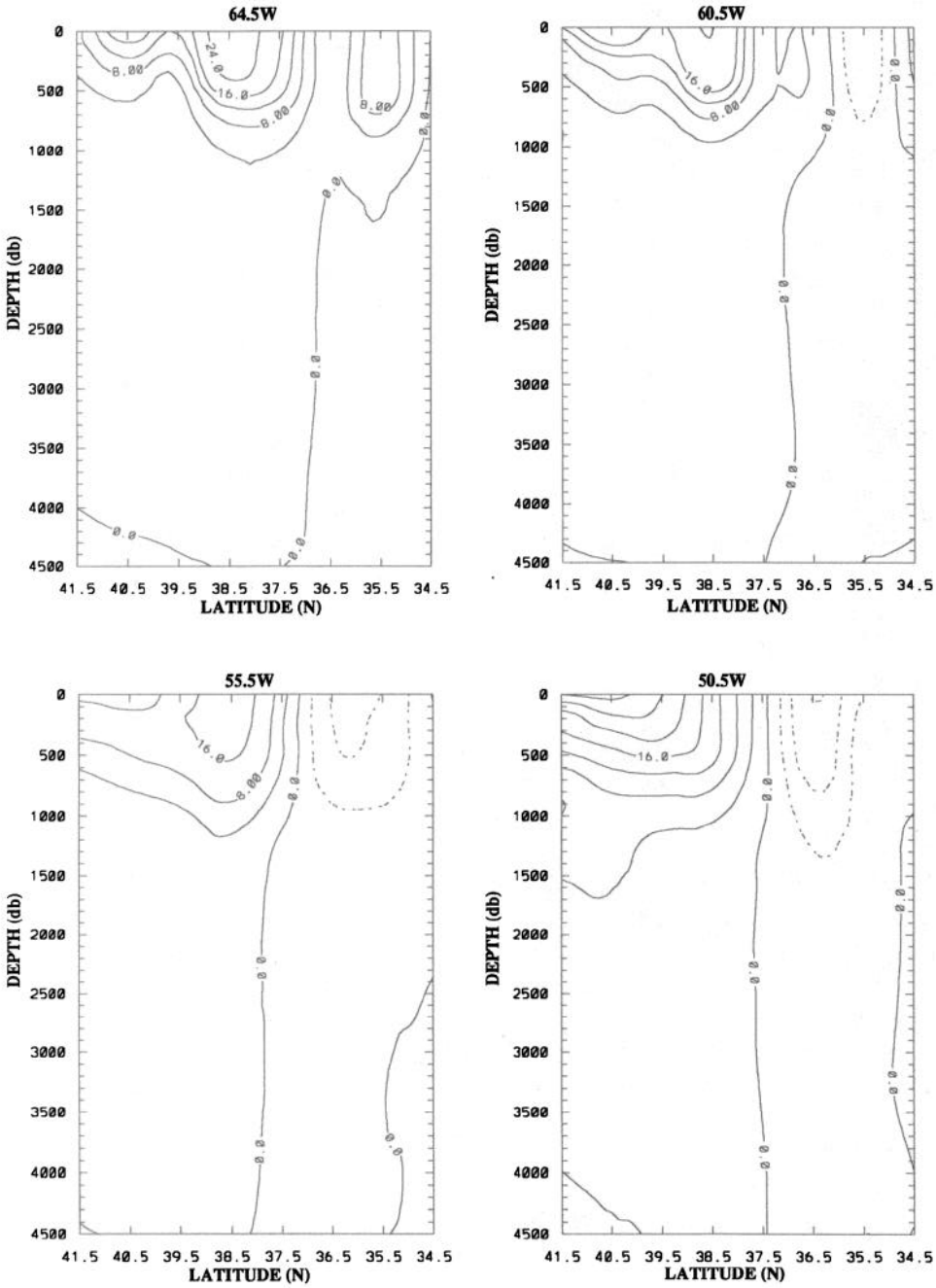

Figure 8. Same as Figure 6 except for the use of a level of no motion at the surface $\sigma_4 = 45.90$. Contour interval is 4 cm sec^{-1}.

eastward flow is approximately at the longitude of the western edge of the Corner Rise (51W), and its eastward path follows the northern edge of the Rise. This deep excursion of the Stream, coupled with the strong baroclinic shear from the hydrographic data that are concentrated to the north of this flow, create an offset of the deep Gulf Stream from the shallow Gulf Stream at this section. In other words, near the eastern edge of our domain it appears that the mean Gulf Stream measured by the floats over the period 1972–1990 had a more southerly position than the mean Gulf Stream position indicated by the 87 years of hydrographic data. Thus, we consider this feature (the offset) to be an artifact of the data sampling. To test whether this feature resulted from significant standard errors in the float data, the geostrophic flows were recalculated using only those float data where the mean velocity exceeded the standard error. Minimal differences were obtained in the velocities produced from this recalculation.

From Figure 8 it is apparent that the strongly sheared upper flow field does not change significantly with the use of a deep level of no motion. However, because of the zero velocity reference field, the northern recirculation and the deep Gulf Stream disappear, reflecting the strong barotropicity of these features. Testimony to its baroclinic strength, the southern recirculation, however, is still evident, although it is restricted to the thermocline waters.

b. Comparable temporal domains. Since the mean hydrographic fields are derived from 87 years of data (1904–1990) and the reference velocities are derived from 19 years of data (1972–1990), potential incompatibilities could arise if the data are marked by strong interdecadel variabilities. To eliminate any incongruity from the differing temporal domains of the collected data, we constructed a new set of mean hydrographic data using only the 19 years of hydrographic station data from 1972–1990. This restriction reduced the total number of hydrographic stations in the domain to 2067. The calculated geostrophic velocities from this calculation are shown for 4 meridional cross sections in Figure 9. The overall pattern of the flow from the earlier calculation (see Fig. 7) remains unchanged. However, the baroclinic structure of the Gulf Stream (on which the hydrographic shear has the most influence) has some noticeable changes. The Gulf Stream is now generally narrower and faster. For example, the maximum eastward velocity at 64.5W has increased from 36 cm/sec to 44 cm/sec. [However, it is noted that the maximum velocity at 50.5W has decreased by 4 cm/sec.] Such changes in the Gulf Stream's width and speed are understandable if we assume that the meandering envelope over 19 years is smaller than the meandering envelope over 87 years. Curiously, we note that the offset flow still exists at the easternmost section. This offset can perhaps be attributed to a sampling bias, whereby the floats near ~50W preferentially sampled a southern excursion of the Gulf Stream over the period 1972–1990. The hydrographic data alone do not support the existence of an offset at this longitude.

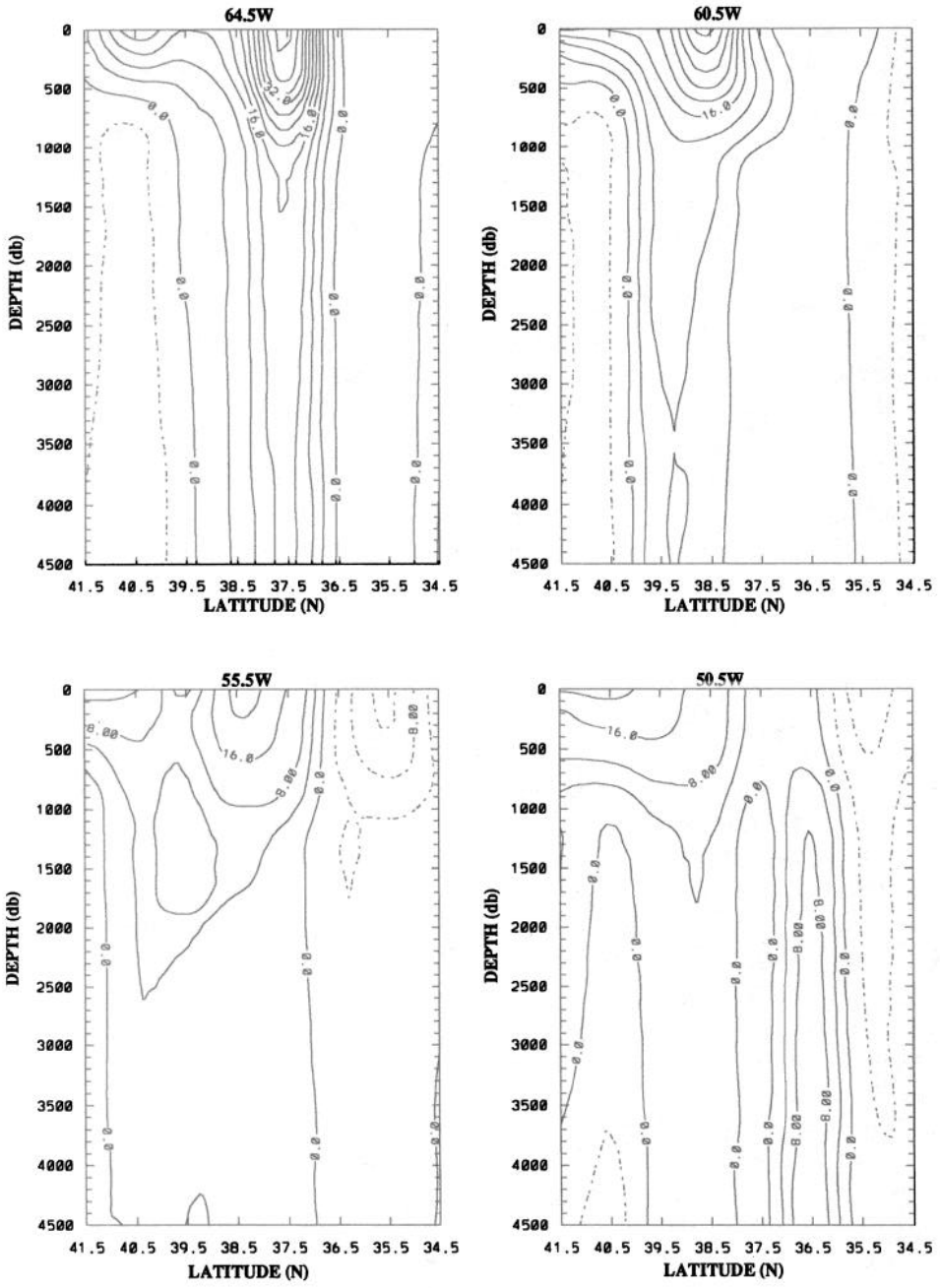

Figure 9. Same as Figure 6 except for the use of 19 years of hydrographic data. Contour interval is 4 cm sec^{-1}.

c. Calculation using isobaric-averaged data. One of the important aspects of this study is that the mean hydrographic fields used in the geostrophic calculations are averaged on isopycnal surfaces. Lozier *et al.* (1994) have shown that significant artifacts can occur in temperature and salinity fields which have been isobaric-averaged. Such biases are strongest in the vicinity of sharply sloping isopycnals. Due to the curvature in the *T-S* relationship, averaging on an isobar in such a locale will create an average temperature and salinity that do not resemble the synoptic values. The difference will be most pronounced at intermediate depths where the curvature in the *T-S* relationship is the greatest. Lozier *et al.* (1994) showed that the Levitus database had artifacts on the order of 1°C along the Gulf Stream front at thermocline depths. In their work they suggested that these hydrographic biases could translate into biases in the velocity shear field. To investigate the magnitude of such biases, in this section the geostrophic calculations are repeated using mean hydrographic fields that have been averaged on isobaric surfaces.

Mean fields of temperature and salinity were constructed on 24 pressure levels using the 87 years of NODC station data, following a similar procedure used in the computation of the isopycnal-averaged fields. These 24 surfaces were chosen to approximately coincide with the isopycnals chosen for the earlier computations. The isobaric-averaged fields also have a nominal resolution of 1 degree. Dynamic heights are calculated from the isobaric-averaged temperature and salinity fields, just as for the isopycnal-averaged fields. Eq. (4) now reduces to the more familiar formulation for the computation of the streamfunction, since the last two terms on the right hand side are zero for an isobaric surface. For the reference surface we chose the deepest isobar (at 4500 m) to be the level of no motion. Because this surface approximately coincides with the $\sigma_4 = 45.90$ surface (with a mean depth of 4419 m in the study area), this calculation mainly differs from that presented in Figure 8 by the averaging process.

Using the isobaric-averaged hydrographic data, the mean density and the mean zonal velocity at each gridpoint for all depths were calculated. These means, along with the means calculated using the isopycnal-averaged data, were interpolated onto a common grid to facilitate a comparison. Figure 10 shows the isopycnal-averaged density and zonal velocity minus the isobaric values at the 64.5W meridional cross section, a representative section. [Note: because of the intersection of isopycnals with the sea surface, data above 100 m depth were not included in this calculation.] The density difference section shows that the largest anomaly ($\sim .12\sigma_t$ units) occurs in the core of the Gulf Stream (upper 1000 m), and that the anomaly is negligible at depth. From the velocity anomaly section we see that the isobaric-averaged fields produce larger velocities in the center of the Stream and smaller velocities on the offshore and onshore flanks, thus influencing the horizontal shear distribution. Local velocity differences are on the order of 2 cm/sec with the largest value approximately 4 cm/sec, which is about 10% of the maximum mean Gulf Stream velocity

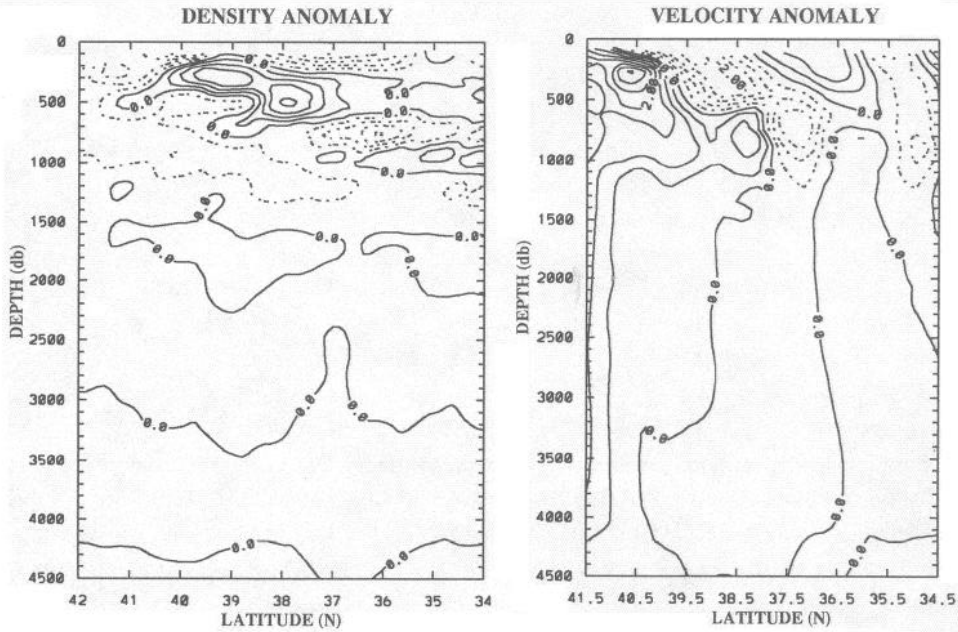

Figure 10. (a) Density and (b) velocity anomalies at 64.5W as a result of using isobaric-averaged hydrographic fields. The contour intervals are $.3\sigma_t$ units and .5 cm sec^{-1} for (a) and (b), respectively.

(~40 cm/sec). Below the Gulf Stream core, the velocity anomaly is also negligible. Although the velocity anomalies can be as high as 10% of the local Gulf Stream mean flow, the net transport change that results from these velocity anomalies, ~3.5 Sv, is insignificant compared to the total transport at that section, which is ~167 Sv (as will be discussed in Section 5). This insignificant change in the net transport indicates that the effect of the isobaric-averaged anomalies is to change the slope of the isopycnal that defines the Gulf Stream baroclinic velocities. At the outer edges of the Stream (where the isopycnal is relatively flat) the anomalies are much reduced and the slopes produced by the two averaging processes converge. Thus, averaging over the entire width of the Stream to produce a transport will show little difference between the two methods. However, there can exist a significant difference in property flux estimates, such as heat and salt, given these local velocity differences and the cross-stream temperature and salinity gradients.

5. Gulf Stream transport

One of the more controversial quantifications of the Gulf Stream has been a measure of its transport. Differences in estimates may be attributed to a variety of factors, including differences in averaging lengths, in geographic locale and/or in measurement techniques. Additionally, long-term variability may account for some

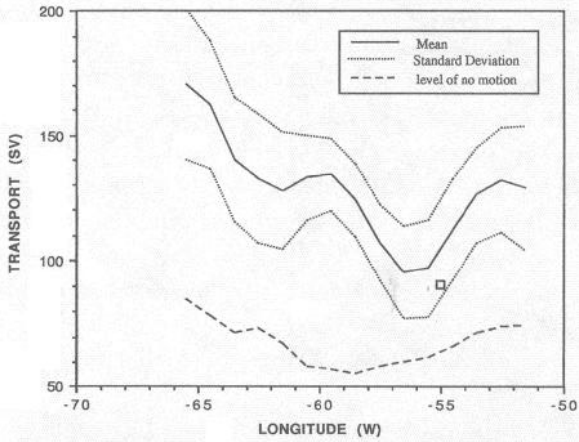

Figure 11. Mean Gulf Stream transport (solid line) and standard deviation envelope (dashed lines) for the calculated transport using the float data. The transport computed by Richardson (1985) at 55W is marked for comparison.

transport differences. In this section, we compute the downstream transport of the Gulf Stream over the selected domain based on the velocity fields generated using 87 years of hydrographic data with (1) the 2000 m floats and (2) with an assumed level of no motion. Our purpose in producing a long-term mean transport estimate is to provide a basis from which transport variability can be measured and to quantify the role of the mean recirculations.

The total downstream transport is calculated from meridional cross sections at every degree of longitude by integrating the zonal velocity over the full depth and width of the section. For the calculation involving the float data we used Monte Carlo simulations to estimate the mean transport and its associated error bounds. Specifically, we generated a series of normally distributed pseudo-random values from the 2000 m mean velocity and its standard error at each 1 degree grid. These random values produce a series of random velocity fields at 2000 m. Each of these random velocity fields is then used as the reference velocity to calculate the absolute geostrophic velocities throughout the water column. Transports were computed for each random simulation and these were then averaged to produce the mean profile shown in Figure 11, along with the standard deviation envelope. Fifty simulations were needed to reach a convergence of the mean transport.

For the transport curve calculated using float data the effect of the recirculations is evident. At the western edge of the domain the transport is quite large due to the intense western cyclonic gyre north of the Stream. The transport decreases precipitously until near 63W. From 62 to 58W there is a moderate rise in the transport due to a small gyre embedded within the larger cyclone. The transport again drops until 57W, the eastern edge of this large cyclonic system. The transport increases again starting at ~56W due to the convergence into the Stream of flow from the second

northern cyclonic gyre, which is east of the NESC. Finally the transport curve begins to drop off after 53W, reflecting the divergence of the Gulf Stream waters into the southern recirculation. Overall, the dominant transport low near 56W reflects the transition area between the two northern cyclonic systems. Interestingly, a minimum in surface transport at approximately this same longitude has been predicted by Kelly and Watts (1994) from a 19-month time series of Geosat altimeter measurements. This coincidence suggests that the northern recirculations are primarily influenced by the barotropic velocity field, as discussed by Hogg *et al.* (1986). Finally, for this calculation it is apparent that the southern recirculation has much less effect than the northern recirculations on the downstream changes of the transport. This can be explained by the broader scale of the southern vs. northern gyres over the scale of our chosen domain.

For the calculation of our streamfunction fields a geographic-coordinate average was used, in contrast to a stream-coordinate average. This choice was made in order to place the Gulf Stream in a geographical context relative to its recirculations. In the computation of such a mean, however, the temporal meandering of the stream has a profound effect. The first order effect is that the stream is understandably widened and weakened, as evidenced by the estimate of the Gulf Stream in Figure 5. The extent of this widening and weakening will be set by the intensity of the temporal meandering of the Gulf Stream. If the Gulf Stream's meandering envelope did not exceed the width of the instantaneous jet the mean transport calculated from a geographic mean would match the mean transport calculated from a synoptic average: the slower flow would cover a broader area, but the transports would be equivalent. For the Gulf Stream however the meandering envelope far exceeds the instantaneous width of the Gulf Stream (Fuglister, 1963; Auer, 1987; Cornillon, 1986). In such a case the recirculations flanking the Gulf Stream can significantly affect the mean Gulf Stream transport calculated using an Eulerian average. Hogg (1992) developed a simple model of a Gulf Stream with flanking westward flows that meandered periodically over a spatial scale of twice the model jet's width. His study showed that an Eulerian-averaged transport is less than the synoptic-averaged transport due to the presence of the recirculating flows. It follows that the transport strength will depend on the extent of the Gulf Stream's meandering and so the question arises as to whether the structure of the transport curve (and indeed the recirculation themselves) is influenced by any longitudinal differences in meandering intensity over our domain. From a five-year study of the Gulf Stream position using oceanographic analysis charts produced from satellite altimetry, Auer (1987) produced a mean position of the Gulf Stream and its standard deviation envelope. From Auer's map (Fig. 3 in Auer, 1987) there is no indication of any minimum or maximum in the meandering intensity over the domain of our study. The only noted change is a slight downstream increase in the meandering envelope. This effect might help to create the divergence noted in our mean fields in the eastern domain. Likewise,

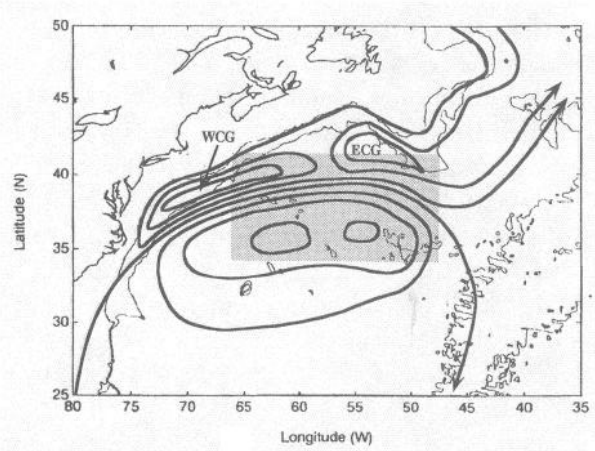

Figure 12. Proposed recirculation scheme for the western North Atlantic. Shaded area shows the domain of the calculations in this work. The western and eastern cyclonic gyres are marked as WCG and ECG, respectively.

Kelly's (1991) study using 2.5 years of Geosat altimeter data shows no extrema in the meandering intensity of the Gulf Stream. While the length of these studies does not approach the termporal record of the hydrographic and/or float data, they do suggest that the transport low at ~56W is not likely an artifact of meandering intensity.

The transport curve shown for the level of no motion calculation is also shown in Figure 11. As expected, the total transport is considerably less in this case since a barotropic component is missing. Interestingly, there does appear to be a minimum in the baroclinic transport centered near 58–59W. This minimum is shifted several degrees to the west of the strong minimum for the curve produced from the calculation with floats, but it does indicate downstream baroclinic transport changes.

Historically, estimates of the Gulf Stream transport have been plentiful (Richardson, 1985), however the vast majority of these estimates have been based on synoptic measurements with time scales on the order of one month. Clearly these estimates are inappropriate for a comparison with the climatological mean presented in this work. Transport estimates based on longer term observations (~1–2 years) have been made, but generally a synoptic average has been used for computing the transport from these observations (Hogg, 1992). As discussed above, it is not valid to compare synoptic averages with geographic averages. Excluding synoptic estimates and synoptic-averaged estimates leaves us with Richardson's (1985) transport estimate at nearly 55W. Richardson estimated the Eulerian mean for the transport using long term current measurements (~two years) from SOFAR float data. His estimate is marked on Figure 11 and is seen to fall within the standard deviation envelope produced by our calculation.

Based on the computations with the float data, the overall transport scheme can be summarized as in Figure 12. This schematic is essentially a modification of the

scheme proposed by Hogg (1992). The major additions are the cyclonic gyre west of 56W and the weak two-cell structure in the southern recirculation. Also, the eastern cyclonic gyre in our scheme occupies a smaller region and is centered further to the east than that proposed by Hogg.

6. Summary

We have constructed the geostrophic velocity field of the Gulf Stream and its recirculations over the domain 66–48W and 34–42N. The calculation was based on mean hydrographic fields constructed from 87 years of hydrographic station data in conjunction with either a 2000 m mean velocity map derived from 19 years of SOFAR float measurements or an assumed level of no motion. Overall, the mean velocity field shows a Gulf Stream that exhibits the baroclinic structures of a synoptic Gulf Stream, including the offshore shifting with depth of its axis. The mean Gulf Stream is flanked by recirculation gyres to both the north and south. The northern recirculation consists of two cyclonic systems and the southern recirculation has two relatively weak cells. The recirculation pattern yields a transport curve with a strong minimum near 56W which is the approximate center of the two northern gyres. The use of a level of no motion for the geostrophic calculations yields an anemic deep flow in terms of strength and structure. The transport estimate from this calculation is approximately one half of that using the float data. Biases in the calculated velocity field are found to be as high as 10% if isobaric-averaged hydrographic fields were used in the calculation instead of isopycnal-averaged hydrographic fields. The net transport changes, however, are found to be minor.

While it was our intent to highlight the features revealed by the new high-resolution hydrographic database, the float velocities actually dominated the vertically-integrated flow field. As mentioned earlier, this is attributed to weak shear below the thermocline, such that the reference velocities are imprinted on all surfaces below ~ 1000 m. Thus, the recirculations seen on the reference surface translate throughout the majority of the water column and dictate the downstream change in the transport. However, while strength of the recirculations produced by this calculation are a result of the float velocities, the existence of them is also supported by the hydrographic data. Additionally, efforts to "clean-up" the float data by matching the time scales and by using only mean velocities that exceed the standard errors, showed little change in the extent and strength of the recirculations.

Finally, we note that for the computation of long-term mean velocities from averaged hydrographic data it can be expected that deep shears will be weak. Thus, efforts to improve our estimates of the flow field and/or transport depend on our ability to produce a statistically meaningful description of long-term absolute velocities at a level in the ocean.

Acknowledgments. The authors are grateful to N. Hogg and B. Owens for their role in the initiation of this work. B. Owens is thanked for providing the SOFAR float data and N. Hogg is

also thanked for his suggestion regarding the Monte Carlo simulation and his helpful review of this manuscript. Support from the National Science Foundation, Grant OCE-9103364 is acknowledged.

REFERENCES

Auer, S. J. 1987. Five-year climatological survey of the Gulf Stream system and its associated rings. J. Geophys. Res., *92,* 11,709–11,726.

Cornillon, P. 1986. The effect of the New England Seamounts on Gulf Stream meandering as observed from satellite IR imagery. J. Phys. Oceanogr., *16,* 386–389.

Csanady, G. T. and P. Hamilton. 1988. Circulation of slope water. Cont. Shelf Res., *8,* 565–624.

Fuglister, F. C. 1963. Gulf Stream '60. Prog. in Oceanogr., *1,* 265–383.

Fukumori, I. and C. Wunsch. 1991. Efficient representation of the North Atlantic hydrographic and chemical distributions. Prog. in Oceanogr., *27,* 111–195.

Hogg, N. G. 1992. On the transport of the Gulf Stream between Cape Hatteras and the Grand Banks. Deep-Sea Res., *39,* 1231–1247.

Hogg, N. G., R. S. Pickart, R. M. Hendry and W. J. Smethie, Jr. 1986. The northern recirculation gyre of the Gulf Stream. Deep-Sea Res., *33,* 1139–1165.

Kelly, K. A. 1991. The meandering Gulf Stream as seen by the Geosat altimeter: Surface transport, position, and velocity variance from 73 to 46W. J. Geophys. Res., *96,* 16,721–16,738.

Kelly, K. A. and D. R. Watts. 1994. Monitoring Gulf Stream transport by radar altimeter and inverted echo sounders. J. Phys. Oceanogr., *24,* 1080–1084.

Levitus, S. 1982. Climatological atlas of the world ocean. NOAA Prof. Paper, 13, 173 pp.

Lozier, M. S., M. S. McCartney and W. B. Owens. 1994. Anomalous anomalies in averaged hydrographic data. J. Phys. Oceanogr., *24,* 2624–2638.

Lozier, M. S., W. B. Owens and R. G. Curry. 1995. The Climatology of the North Atlantic. Prog. in Oceanogr. (in press).

Martel, F. and C. Wunsch. 1993. The North Atlantic circulation in the early 1980s—An estimate from inversion of a finite-difference model. J. Phys. Oceanogr., *23,* 898–924.

Mercier, H. 1989. A study of the time-averaged circulation of the western North Atlantic by simultaneous nonlinear inversion of hydrographic and current meter data. Deep-Sea Res., *36,* 297–313.

Mercier, H., M. Ollitrault and P. Y. Le Traon. 1993. An inverse model of the North Atlantic general circulation using Lagrangian float data. J. Phys. Oceanogr., *23,* 689–715.

Owens, W. B. 1991. A statistical description of the mean circulation and eddy variability in the northwestern Atlantic using SOFAR floats. Prog. in Oceanogr., *28,* 257–303.

Richardson, P. L. 1985. Average velocity and transport of the Gulf Stream near 55W. J. Mar. Res., *43,* 83–111.

Schmitz, W. J., Jr. and M. S. McCartney. 1993. On the North Atlantic Circulation. Rev. of Geophys., *31,* 29–49.

Worthington, L. V. 1976. On the North Atlantic Circulation. The Johns Hopkins Oceanographic Studies, *6,* 110 pp.

Wunsch, C. 1978. The North Atlantic general circulation west of 50W determined by inverse methods. Rev. of Geophys. Space Phys., *16,* 583–620.

Wunsch, C. and B. Grant. 1982. Towards the general circulation of the North Atlantic Ocean. Prog. in Oceanogr., *1,* 1–59.

Zhang, H. M. and N. Hogg. 1992. Circulation and water mass balance in the Brazil basin. J. Mar. Res., *50,* 385–420.

Received: *3 January, 1995;* revised: *12 July, 1995.*